The Journal of Neuroscience, June 1, 1996, *16*(11):3661–3671

Identification and Characterization of a Ca^{2+}-Sensitive Nonspecific Cation Channel Underlying Prolonged Repetitive Firing in *Aplysia* Neurons

Gisela F. Wilson,[1] Frank C. Richardson,[1] Thomas E. Fisher,[1] Baldomero M. Olivera,[2] and Leonard K. Kaczmarek[1]

[1]*Department of Pharmacology, Yale University, New Haven, Connecticut 06510, and* [2]*Department of Biology, University of Utah, Salt Lake City, Utah 84112*

The afterdischarge of *Aplysia* bag cell neurons has served as a model system for the study of phosphorylation-mediated changes in neuronal excitability. The nature of the depolarization generating the afterdischarge, however, has remained unclear. We now have found that venom from *Conus textile* triggers a similar prolonged discharge, and we have identified a slow inward current and corresponding channel, the activation of which seems to contribute to the onset of the discharge. The slow inward current is voltage-dependent and Ca^{2+}-sensitive, reverses at potentials slightly positive to 0 mV, exhibits a selectivity of K ≅ Na ≫ Tris > *N*-methyl-D-glucamine (NMDG), and is blocked by high concentrations of tetrodotoxin. Comparison of these features with those observed in channel recordings provides evidence that a Ca^{2+}-sensitive, nonspecific cation channel is responsible for a slow inward current that regulates spontaneous repetitive firing and suggests that modulation of the cation channel underlies prolonged changes in neuronal response properties.

Key words: Ca^{2+}-activated nonspecific cation channel; slow inward current; ion channel modulation; afterdischarge; bursting; Aplysia *bag cell neurons;* Conus textile

Changes in slow inward currents are a powerful and widespread mechanism for producing prolonged alterations in the electrical activity of neurons. Slow inward currents influence the number and pattern of action potentials elicited in response to stimulation and, even more basically, determine the presence and level of spontaneous electrical activity. A role for slow inward currents in providing the depolarizing drive underlying endogenous bursting has been suggested in a number of mammalian (Lanthorn et al., 1984; Stafstrom et al., 1985; Alonso and Llinas, 1989) and molluscan neurons (Wilson and Wachtel, 1974; Eckert and Lux, 1976; Partridge et al., 1979; Hofmeier and Lux, 1981; Lewis, 1984; Kramer and Zucker, 1985; Swandulla and Lux, 1985), and slow inward currents also may play a role in the generation of epileptiform activity in the hippocampus (Hoehn et al., 1993) and pacemaker potentials in the heart (Colquhoun et al., 1981; Reuter, 1984).

One particularly dramatic example of a long-lasting change in spontaneous activity is found in the bag cell neurons that mediate egg-laying behaviors in *Aplysia*. Bag cell neurons are located in two symmetric clusters, each containing from 200 to 400 neurons, at the juncture of the abdominal ganglion and the pleuroabdominal connective nerve. Normally these neurons are silent; however, brief stimulation of the presynaptic nerve triggers a depolarization that causes an ~30 min period of spontaneous action potentials referred to as the afterdischarge (Kupfermann and Kandel, 1970; Kaczmarek et al., 1978). The afterdischarge differs from the bursting behavior described for other neurons in that action potentials typically are not clustered and that, apart from a gradual decline, there is little variation in the underlying depolarization once the afterdischarge is initiated. In addition, the afterdischarge is followed by a refractory period lasting ~18 hr, during which further electrical stimulation fails to depolarize cells and fails to trigger an afterdischarge (Kupfermann and Kandel, 1970; Kauer and Kaczmarek, 1985).

We now present evidence that activation of a slow inward cation current may provide the depolarizing drive underlying the afterdischarge. This current normally is not detected in single bag cell neurons and has not been examined in intact ganglia because of the extensive electrical coupling between neurons. To allow the cation current to be examined in single bag cell neurons, we induced the current using an extract of venom from *Conus textile* (CtVm) that, in intact ganglia, triggers a discharge similar to that observed after electrical stimulation. *Conus textile* is a member of the marine snail genus that has provided a number of neurotoxins that act on nicotinic acetylcholine receptors, voltage-dependent sodium (Na) channels, and neuronal N-type Ca channels (for review, see Gray et al., 1988; Olivera et al., 1990). The inward cation current observed after treatment with CtVm is voltage-dependent and Ca^{2+}-sensitive, inactivates slowly over a period of minutes, is blocked by high concentrations of tetrodotoxin (TTX), and is carried by both monovalent and divalent cations. In previous work (Wilson and Kaczmarek, 1993), we described the modulation of a cation channel by both serine/threonine and tyrosine phosphorylation systems. We now also show that the properties of this cation channel correspond closely to that of the slow inward current observed in whole-cell experiments, a result which sug-

Received Aug. 28, 1995; revised March 13, 1996; accepted March 15, 1996.

This work was supported by a National Institutes of Health postdoctoral fellowship (F32 NS08986) to G.F.W. and a grant from National Institutes of Health (NS18492) to L.K.K.

Correspondence should be addressed to Leonard K. Kaczmarek, Department of Pharmacology, Yale University, 333 Cedar Street, New Haven, CT 06510.

Dr. Wilson's present address: Laboratory of Genetics, University of Wisconsin, Madison, WI 53706.

Dr. Fisher's present address: Centre for Research in Neuroscience, Montréal General Hospital and McGill University, 1650 Cedar Avenue, Montréal, Québec, Canada H3G 1A4.

gests that modulation of bag cell neuron–cation channels is crucial to the initiation of the prolonged discharge by CtVm.

MATERIALS AND METHODS

Cell preparation

Adult *Aplysia californica* (Alacrity Marine Biological Services, Redondo Beach, CA) were anesthetized by injecting isotonic $MgCl_2$, and the abdominal ganglia were excised along with the pleuroabdominal connective nerves. Abdominal ganglia used in extracellular recording experiments were transferred immediately to artificial seawater (ASW) containing (in mM): 460 NaCl, 10.4 KCl, 11 $CaCl_2$, 55 $MgCl_2$, and 10 HEPES, pH 7.8 (NaOH).

Primary cultures of bag cell neurons were obtained as described previously (Kaczmarek et al., 1979) by treating the abdominal ganglia in neutral protease (20 mg/ml; Boehringer Mannheim, Indianapolis, IN) for 18 hr at room temperature (~22°C). Bag cell neuron clusters then were removed from the surrounding connective tissue, dissociated by gentle trituration with a fire-polished Pasteur pipette, and plated onto 35 mm tissue culture dishes at a density of 10–20 neurons per dish. Cultures were maintained at 14°C in ASW supplemented with glucose (1 mg/ml), penicillin (100 U/ml), and streptomycin (0.1 mg/ml) for 1–4 d before recording.

Electrophysiology

The activity of bag cell neurons in intact abdominal ganglia was recorded extracellularly in a recording chamber maintained at 14°C using suction electrodes placed over bag cell neuron clusters. Afterdischarges were electrically stimulated by passing a brief train of pulses (8–20 V, 2.5 msec at 6 Hz for ~10 sec) through a second suction electrode placed on the ipsilateral pleuroabdominal connective nerve. Data were stored on videocassette tapes and replayed on a Grass Instruments chart recorder. The activity of single-cultured bag cell neurons was recorded intracellularly using an Axoclamp amplifier (Axon Instruments, Foster City, CA). For single-electrode voltage-clamp and current-clamp experiments, pulse generation and data acquisition were performed using a 386 IBM/AT-compatible computer and Fastlab software. Pipettes were filled with 2 M potassium acetate and had resistances of 12–20 MΩ. For whole-cell current–voltage relations, current values were measured at the end of the response to each 3 sec test pulse to the indicated voltage. A 3 sec interval separated successive test pulses; 1–2 min separated each family of test pulses for successive current–voltage relations. Single-channel currents of patches excised from single-cultured bag cell neurons were recorded using a List EPC-7 amplifier, low-pass-filtered at 3 kHz, and stored on videocassettes. Data acquisition and analysis were performed using software written in Axobasic (Axon Instruments). Unless otherwise noted, the solution facing the extracellular side of the membrane was ASW, and the solution facing the intracellular side contained (in mM): 500 K-aspartate, 70 KCl, 0.77 $CaCl_2$, 1.2 $MgCl_2$, 10 HEPES, 11 glucose, 0.77 EGTA, 10 glutathione (a reducing agent), 5 ATP (grade 2 disodium salt; Sigma, St. Louis, MO), and 0.1 GTP (type 3 disodium salt; Sigma), pH 7.3 (KOH). Pipettes were coated with SYLGARD and had resistances ranging from 3–6 MΩ with the exception that, in outside/out patch experiments, higher resistance pipettes (8–15 MΩ) were used to minimize the number of channels per patch. Pipette junction potentials were nulled immediately before seal formation. Channel amplitudes were measured by subtracting straight lines fitted by eye to open and closed current levels for 0.5–2 sec segments of activity. Because of the low probability of encountering single cation channels, especially in outside/out patches, and because of the wide range of open probabilities (P_o) observed for cation channels in control conditions, some experiments relied on visual comparisons of P_o. A clear change in the current level at which the predominant activity occurred was judged as indicating a corresponding change in the average P_o. In whole-cell patch-clamp experiments examining the Ca^{2+}-dependence of the depolarization, the intracellular solution in the patch pipette (1–2 MΩ) contained 5 mM $MgCl_2$ and either 0.2 mM EGTA and 0 mM $CaCl_2$; 20 mM EGTA and 4.14 mM $CaCl_2$ (for a calculated free Ca^{2+} concentration of 3.5×10^{-8} M); or 40 mM EGTA and 4.14 mM $CaCl_2$ (for a calculated free Ca^{2+} concentration of 1.5×10^{-8} M). Calcium concentrations were calculated according to Chang et al. (1988). All experiments were performed at room temperature (~22°C).

Ion substitution. In ion substitution experiments, the Na^+ or Ca^{2+} of ASW was substituted with an equimolar amount of the test cation. Test solutions were perfused using gravitational flow. In isolated patch experiments, test solutions were applied using a multibarrel perfusion system as described by Yellen (1982), by which patches were moved from the mouth of one barrel to the next permitting a nearly instantaneous change in solutions at the face of the patch. In experiments examining the Ca^{2+}-dependence of single-channel activity, the free Ca^{2+} of the intracellular solution was adjusted to the desired level by including 0.77 mM EGTA and either 0.77, 0.385, 0.07, or 0 mM $CaCl_2$ for 10^{-6}, 10^{-7}, 10^{-8}, and 10^{-9} free Ca^{2+} concentrations, respectively.

Conus textile *venom.* CtVm was obtained and prepared as described in Cruz et al. (1976) and Hillyard et al. (1989). CtVm was applied by pipetting an aliquot into the recording solution to obtain the stated final concentrations. In all experiments with intact ganglia, the venom remained in the bath for the duration of the discharge; for the assessment of refractoriness involving multiple applications, CtVm was washed from the bath immediately after the termination of a discharge.

RESULTS

CtVm effects on bag cell neurons of intact abdominal ganglia

In their resting state, bag cell neurons of acutely isolated abdominal ganglia display little or no spontaneous activity. As shown in the extracellular recordings of Figure 1*A* (*top*), however, brief electrical stimulation of the pleuroabdominal nerve innervating the bag cell neuron cluster triggers a long-lasting period of spontaneous repetitive action potentials ~30 min in duration, as has been described previously (Kupfermann and Kandel, 1970; Kaczmarek et al., 1978). We have found that CtVm (100 μg/ml), when bath-applied to resting cells (shown by the *arrow* in Fig. 1*A*, *bottom*), is capable of triggering a similar prolonged discharge. The bag cell neuron response to CtVm could occur within seconds, although typically it occurred within 1–5 min after addition of the extract. The discharge elicited by CtVm was comparable to that observed in response to electrical stimulation both in duration and in the exhibition of characteristic fast and slow firing phases ($n = 6$). CtVm further mimicked electrical stimulation in that CtVm-induced discharges were followed by a prolonged refractory period. Refractoriness was assessed using either electrical stimulation or CtVm at times ranging from 30 min to 2 hr after completion of the first discharge. Longer times were not tested. The refractoriness induced by electrical stimulation blocked the ability of CtVm to induce a prolonged discharge ($n = 4$), and, conversely, the refractoriness induced by CtVm blocked the ability of electrical stimulation to induce a prolonged discharge ($n = 4$).

CtVm effects on isolated bag cell neurons

With the aim of characterizing the ionic mechanism underlying the onset of the CtVm-induced discharge, we examined the effects of CtVm on isolated neurons to determine whether afterdischarge-like activity could be elicited. As shown in Figure 1*B*, CtVm applied to single bag cell neurons produced an abrupt depolarization, which was often accompanied by a prolonged burst of action potentials. In 39 cells examined, CtVm (100 μg/ml) produced a mean peak depolarization of 29.7 ± 2.5 mV from a starting resting potential averaging −48.0 ± 1.9 mV. In approximately one-third of the cells, the depolarization was preceded by a brief hyperpolarization ranging from 5 to 22 mV in magnitude. Although in some cases the response to the extract was immediate (i.e., within seconds), the response usually occurred within 1–5 min after application and decayed gradually over a period ranging from 5 to 30 min. Similar results were obtained with concentrations of extract as low as 5 μg/ml. As observed for the CtVm-induced discharge in intact ganglia, reapplication of CtVm failed to elicit subsequent depolarizations even after washes of extended duration (e.g., 30 min; $n = 3$). The "King Kong" peptide, isolated

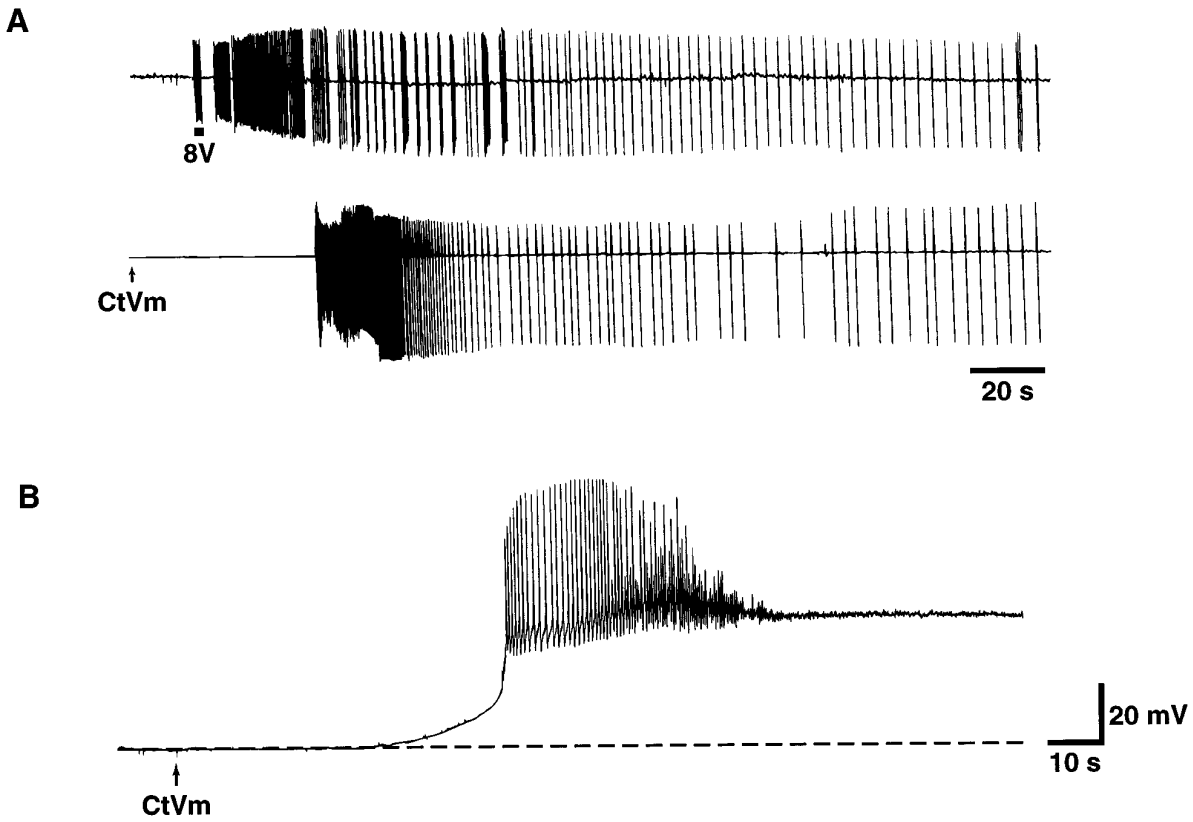

Figure 1. Effect of CtVm on bag cell neurons of intact abdominal ganglia and single bag cell neurons isolated and maintained *in vitro*. *A*, Comparison of electrically stimulated and CtVm-induced discharges recorded from bag cell neurons of intact abdominal ganglia. *Top*, Discharge triggered by a train of electrical pulses (8 V, 6 Hz) applied to the pleuroabdominal nerve with a suction electrode for the duration indicated by the *bar* immediately below the trace. *Bottom*, Discharge triggered by bath application of CtVm (100 μg/ml). *B*, Voltage response of a single-cultured bag cell neuron to application of CtVm (100 μg/ml).

from CtVm by Hillyard et al. (1989), failed to reproduce any of the above effects ($n = 4$; data not shown), suggesting that the component of CtVm acting on bag cell neurons is a novel toxin.

In voltage-clamp experiments, treatment with CtVm resulted in the activation of two voltage-dependent inward currents normally not observed in the current–voltage relations of bag cell neurons. Figure 2*A* shows typical currents elicited in response to voltage steps to −30 mV from a holding potential of −70 mV before (*top trace*) and immediately after (*bottom trace*) application of CtVm. The average control and CtVm current–voltage relations, obtained by measuring the current amplitudes at the end of the response to test pulses to the indicated voltages, are shown in Figure 2*B* ($n = 6$). Pharmacological evidence suggests that the change in the current–voltage relation is attributable to the activation of two independent currents. At negative potentials, application of CtVm (100 μg/ml) caused the appearance of a current with properties matching those of inwardly rectifying potassium (K_{IR}) currents. The contribution of the K_{IR} current could be eliminated from the response to CtVm by bath application of either 10 or 20 mM CsCl ($n = 4$; Fig. 2*C*, *left*) and seemed to account for the brief hyperpolarizations sometimes observed in response to the extract. Treatment with CtVm also caused the appearance of a negative slope resistance region in the steady-state current–voltage relation. The corresponding current, which we have shown is a cation current (see below) and refer to as I_{CAT}, was maximally activated near −40 mV and was unaffected by the presence of up to 20 mM CsCl, but it could be blocked with high concentrations of TTX (100 μM; $n = 22$; Fig. 2*C*, *right*). In addition, no depolarizations were observed when CtVm was applied in the presence of TTX ($n = 3$; data not shown).

Identification of a CtVm-regulated cation channel

Patch-clamp experiments were performed to identify the channel carrying the cation current. No channels carrying noninactivating inward current were observed in cell-attached patches when ASW served as the extracellular solution. In contrast, cation channels were observed in 10–20% of patches excised into the inside/out configuration. As has been described previously (Wilson and Kaczmarek, 1993), after patch excision, cation channels were found in either a bursting or continuously active gating mode. The bursting mode (see Fig. 4*B*, *top trace*) is distinguished from the continuously active mode (see Fig. 4*A*, *top trace*) by the occurrence of long closed times lasting tens of seconds to minutes. An examination of closed-time distributions of channels in the bursting mode reveals a distinct population of closed events of long duration that is not observed in closed-time distributions of continuously active channels. Otherwise, the event distributions for channels in the two gating modes are indistinguishable (Wilson and Kaczmarek, 1993).

Figure 3*A* shows steady-state recordings of a continuously active cation channel at holding potentials of −40, −60, −80, and −100 mV. Although the P_o of cation channels varied considerably from patch to patch, the fraction of time cation channels spent in the open state clearly decreased at increasingly hyperpolarized potentials. The average voltage-dependence of the P_o and the average open channel current–voltage relation obtained for seven

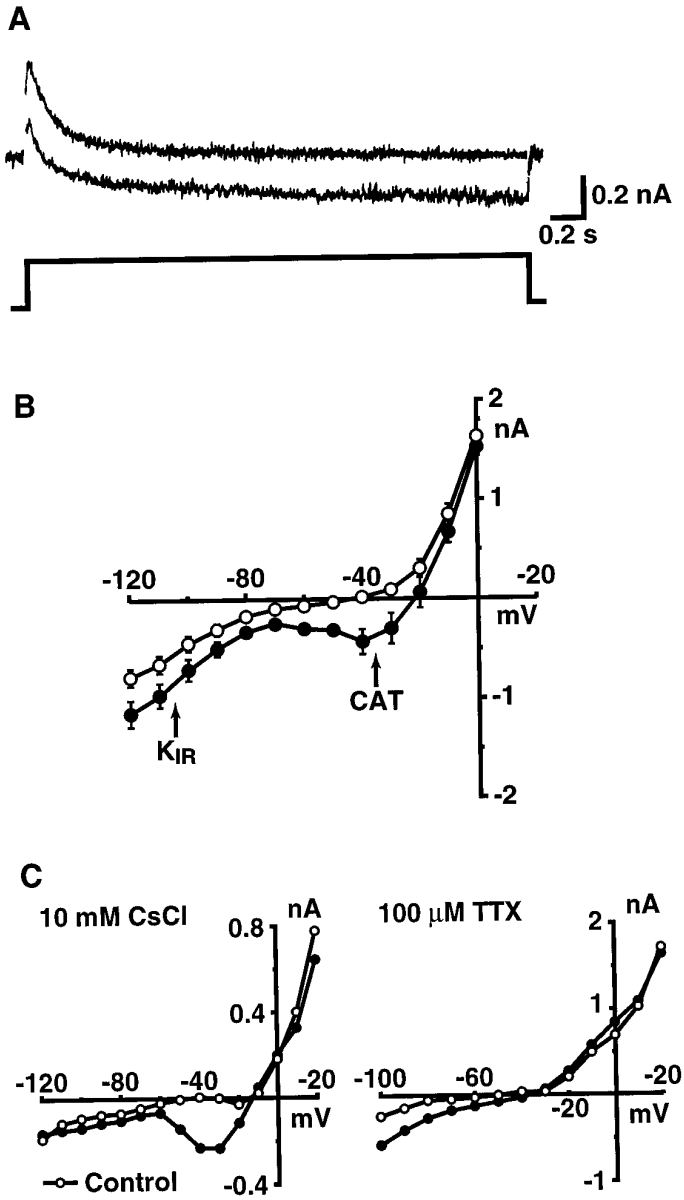

Figure 2. Treatment with CtVm results in the activation of two voltage-dependent inward currents. *A*, Representative current traces elicited in response to 3-sec-long voltage steps to −30 mV from a holding potential of −70 mV before (*top trace*) and after (*bottom trace*) application of CtVm (100 μg/ml). For display, linear leakage and capacitative components have been subtracted. *B*, Average current–voltage relations observed in bag cell neurons before (○) and after (●) application of CtVm (100 μg/ml; $n = 6$). *C*, Pharmacological identification and isolation of K_{IR} and cation current components of the response to CtVm. *Left*, representative current–voltage relation before (○) and after (●) application of CtVm and 10 mM CsCl. *Right*, representative current–voltage relation before (○) and after (●) application of CtVm and 100 μM TTX. In *B* and *C*, currents were measured during the steady-state portion of the response to a step to the indicated voltage from a holding potential of −60 mV.

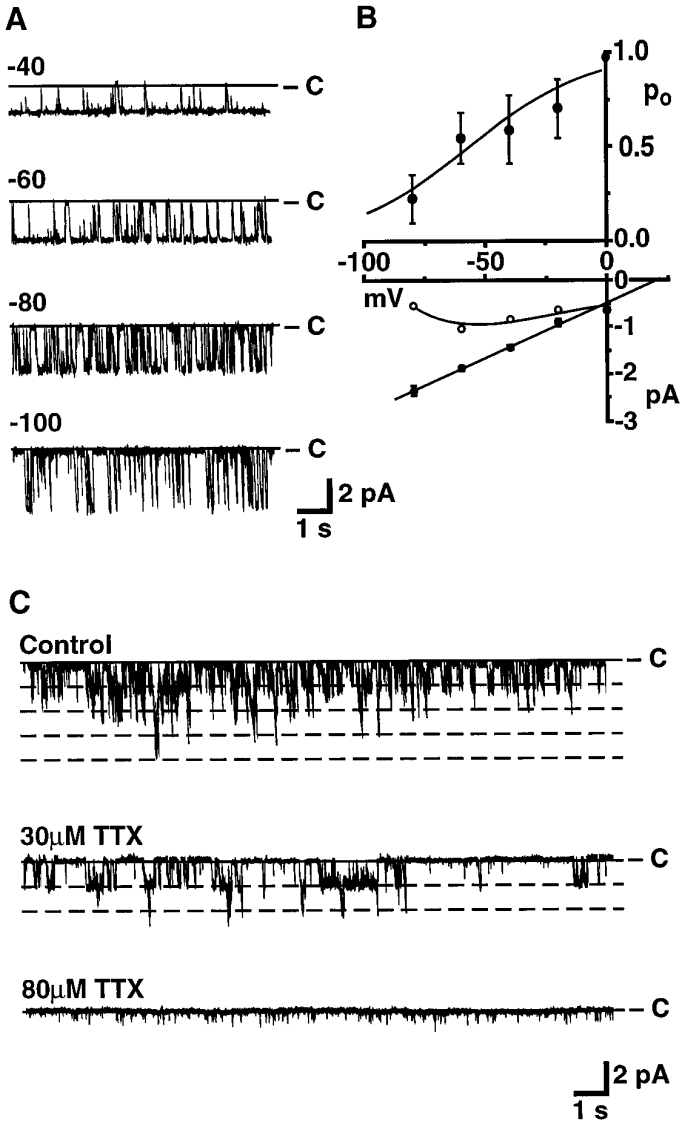

Figure 3. Voltage dependence and TTX block of cation channel activity in excised patches of bag cell neuron membrane. *A*, Sample steady-state recordings of cation channel activity in an excised inside/out patch held at the potentials indicated above each trace. Downward deflections correspond to inward current. *B*, Average open-channel current–voltage relation (*bottom*, ●) and voltage-dependence of the P_o (*top*) from seven inside/out patches containing single cation channels. The *open circles* were obtained from the relation $I = i \times P_o$ applied to each data point, where i represents the open-channel current. A Boltzmann function was fit to the P_o points using a Simplex fitting routine with the minimax criterion for error minimization (pCLAMP6); other curves were fit to the points by eye. *C*, TTX block of cation channel activity in an excised outside/out patch held at −60 mV. At the start of the experiment, four current levels were observed, suggesting the presence of four cation channels in the patch. The activity remaining at 80 μM TTX seemed to be attributable predominantly to the presence of a smaller conductance channel, which sometimes was observed in inside/out patches.

patches containing only one channel are plotted in Figure 3*B* (*top* and *bottom*, respectively). The slope conductance of the cation channel in inside/out patches, as determined by a straight-line fit to the averaged points, was 29.4 pS, and the reversal potential of the single-channel current appeared more positive than that of the whole-cell current, a result which is discussed in greater detail in association with Figure 6 and in Discussion. The P_o increased as the membrane potential was depolarized from −120 mV, reaching maximal levels near 0 mV. A Boltzmann function fit to the averaged points (*solid curve*, Fig. 3*B*, *top*) indicated a midpoint of activation at −56.0 mV and a slope of 24.6 mV per e-fold change in P_o. To determine the expected contribution of the cation channel to the whole-cell current–voltage relation, the open circles in Figure 3*B* were obtained from the relation $I = i \times P_o$

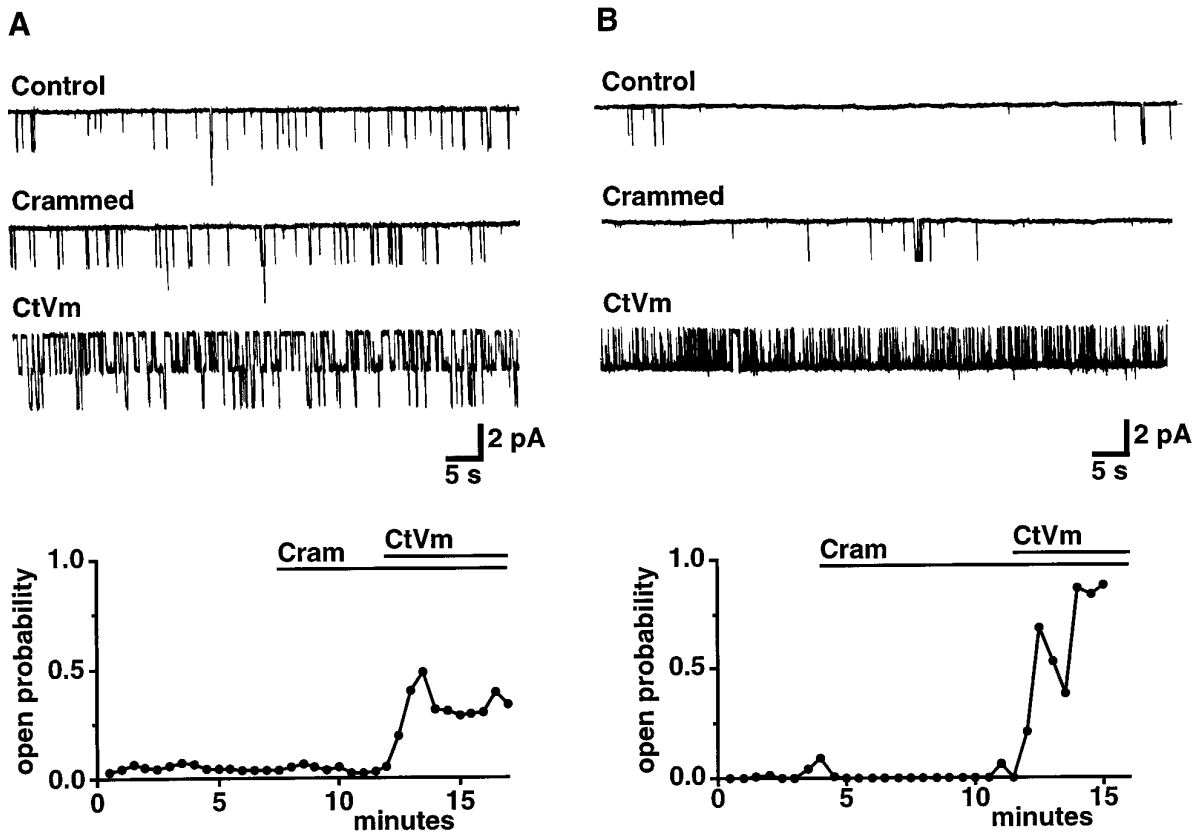

Figure 4. Effect of CtVm on cation channels in either a continuously active (*A*) or bursting (*B*) gating mode. Cation channels were identified and characterized by excising patches into intracellular solution [containing (in mM): 500 K-aspartate, 70 KCl, 0.77 $CaCl_2$, 1.2 $MgCl_2$, 10 HEPES, 11 glucose, 0.77 EGTA, and 10 glutathione, pH 7.3 (KOH)], and then the channels were reinserted ("crammed") into bag cell neurons before application of CtVm (100 μg/ml). In both *A* and *B*, traces show representative activity recorded at a holding potential of −60 mV in control conditions, after cramming, and after application of CtVm, as indicated. The time dependence of the changes in P_o are shown in the plots below. Data points represent the P_o measured for successive 30 sec intervals. For the patch shown in *A*, which appeared to contain two channels, the plotted P_o is the sum of the P_o obtained at each level divided by two. Bursting and continuously active channels were distinguished by the presence of long-lived closures in the activity of bursting channels, as described previously (Wilson and Kaczmarek, 1993). A reasonable fit of the closed-time distribution of bursters requires the use of additional exponentials that describe the long-lived closures. These exponentials are not required when fitting the closed-time distributions of continuously active channels.

applied to each of the average data points; the dashed curve was fit to the derived points by eye. The voltage-dependent behavior of the cation channel corresponds reasonably to that of the whole-cell current (see Discussion).

Cation channels also were blocked by concentrations of TTX similar to those required to block the whole-cell current. For the outside/out patch shown in Figure 3*C*, four current levels were observed in control conditions, suggesting the presence of four cation channels in the patch. After application of TTX (30 μM), only two levels of current were observed, and channel activity appeared completely blocked when TTX was increased to a final concentration of 80 μM. The remaining activity was predominantly attributable to the presence of a smaller conductance channel that was sometimes also observed in inside/out patches. TTX similarly blocked cation channel activity in the three other patches tested; reversibility of the TTX effect was not examined.

The above results suggest that the ~30 pS channel underlies the depolarization and whole-cell cation current observed in response to CtVm and that, because CtVm activates the whole-cell current, CtVm also should increase the cation channel P_o. To test this possibility, cation channels were localized and their gating mode in control conditions characterized by excising patches into a bath containing intracellular solution. Patches then were reinserted ("crammed") (Kramer, 1990) into the cell of origin before application of CtVm. Typical recordings from two patches held at −60 mV and containing cation channels in either a continuously active or a bursting mode are shown at the top of Figure 4, *A* and *B*, respectively. The P_o observed for the cation channels during successive 30 sec intervals is plotted immediately below. No change in activity was observed for either the continuously active or bursting channels as a consequence of cramming. Application of CtVm, however, produced a dramatic increase in P_o for cation channels in either mode (n = 9 of 11 and 5 of 6 patches tested containing continuously active and bursting channels, respectively). As shown for the patch of Figure 4*A*, which contained two continuously active channels with an average low starting P_o of 0.04, CtVm increased the average P_o to 0.34, an increase more than eightfold. An even larger increase in P_o was observed after application of CtVm to "crammed" patches containing bursting channels. CtVm increased the P_o of the bursting channel of Figure 4*B* from an average starting value of 0.01 to an average final value of 0.86. Because no change in the current amplitudes of cation channels was observed either as a function of cramming or as a function of CtVm application, the changes in P_o cannot be accounted for by a change in the potential of the crammed patch. In summary, the patch configurations examined included cell-

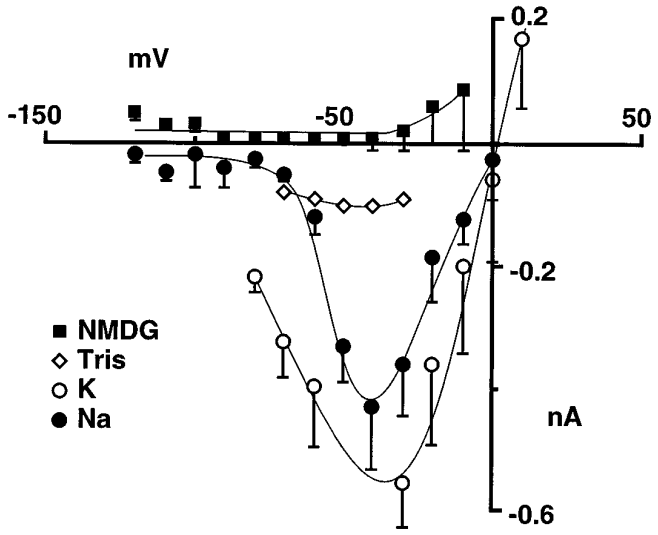

Figure 5. Average current–voltage relations of the whole-cell cation current in ion-substituted seawater as measured in a single-electrode voltage clamp. The Na^+ of ASW was substituted with an equimolar amount of the indicated cations. The cation current was isolated from other bag cell neuron currents by subtracting the current–voltage relation obtained in steady-state conditions in the presence of CtVm and TTX from that obtained in the presence of CtVm alone. *N* equals 7, 3, 1, and 3 for Na^+, K^+, Tris (see text), and NMDG containing ASW, respectively.

attached patches with bath-applied CtVm, cell-attached patches with CtVm included in the pipette solution, and outside/out, inside/out, and crammed inside/out patches. The cation channel was the only channel encountered that carried inward current, was blocked by TTX, and displayed an increase in P_o in response to CtVm.

The patch configuration in which a neuropeptide is observed to have an effect can indicate whether the peptide interacts directly or indirectly with the channel under study. In the above crammed inside/out patches, an increase in P_o was observed even though bath-applied CtVm did not have direct access to the extracellular face of cation channels because of the presence of the patch pipettes. This result suggests that binding to the channel is not required and, therefore, that the effect of CtVm is mediated by an intracellular messenger(s). The fact that the activity of K_{IR} channels, examined in cell-attached patches with 570 mM K^+ in the pipette, increased after bath application of CtVm ($n = 3$; data not shown) further supports the involvement of intracellular messengers in the action of CtVm.

Ion selectivity of the CtVm-induced macroscopic current

To further compare the whole-cell cation current and cation channel, we examined their selectivity for various ions. In experiments examining the whole-cell cation current (Fig. 5), the contribution of other bag cell neuron currents was minimized by measuring the TTX-sensitive component of the CtVm response. This was accomplished by subtracting the steady-state current–voltage relation obtained in the presence of CtVm and TTX from that obtained in the presence of CtVm alone. Because the current corresponding to the classic voltage-sensitive sodium current inactivates rapidly, it does not contribute to this difference current, which is measured at the end of 3 sec voltage commands. Given the gradual decay of the CtVm-induced current, this procedure allowed only a single test solution to be assessed for each cell. Although the difference current appeared to provide the clearest measure of the cation current, the difference current still may be contaminated by a gradual rundown of other bag cell neuron currents active late in the response to each test pulse.

As shown in Figure 5, in normal ASW containing 460 mM Na^+, the reversal potential of the average difference current was near 1.5 mV. The proximity of the reversal potential to zero suggested that the cation current was nonselective relative to classic Na, Ca, and K channels. As has been noted for other nonspecific cation channels (for review, see Partridge and Swandulla, 1988), K^+ ions appeared to carry the current at least as well as Na^+ ions. For these experiments, 10 mM Cs^+ was included to minimize the contribution of the K_{IR} current at high K^+ concentrations. Little change in the reversal potential of the average current–voltage relationship was observed when the Na^+ in ASW was replaced by an equimolar amount of K^+ ($n = 3$). In contrast, when Tris replaced the Na^+ of ASW (Tris-ASW), the TTX-sensitive cation current was detected in only 4 of the 26 cells tested and was markedly smaller when observed. The CtVm-induced depolarizations in Tris-ASW also appeared briefer than those observed in normal ASW (lasting only 1–2 min; $n = 4$). Given the time needed to obtain the TTX difference current, the brevity of the CtVm response in Tris-ASW may account for our failure to observe the CtVm-induced cation current in most cells when Tris was the major cation. No inward cation current was observed when Na^+ was replaced with an equimolar amount of NMDG ($n = 3$), suggesting either that NMDG was not measurably permeant or that, as in Tris-ASW, the current was activated only briefly. The outward current seen at voltages positive to −40 mV is most likely attributable to a slow rundown or inactivation of another current that occurs during the time needed to obtain the difference current. The activation threshold for the outward current seems to correspond with that of a potassium current.

Ion selectivity of the cation channel

The relative permeability of the above ions also was assessed in cation channel recordings from outside/out patches of bag cell neuron membranes. In contrast to the whole-cell experiments, the ongoing channel activity of excised outside/out patches allowed multiple solution changes to be made for a single patch. To permit a comparison of whole-cell and single-channel measurements, external solutions consisted of ASW with an equimolar amount of the test ion replacing Na^+. Sample recordings of channel activity at a holding potential of −60 mV are shown in Figure 6*A* for each test solution, and the corresponding average open-channel current–voltage relations are shown in Figure 6*B*. Neither the amplitude of the open-channel current recorded at −60 mV nor the single-channel conductance changed appreciably when the solution perfusing the outside of the patch was changed to ASW in which K^+ replaced Na^+. In K^+-ASW, the average single-channel conductance in outside/out patches (measured between −100 and 0 mV) was 30.5 ± 1.5 pS ($n = 6$) compared with the 29.1 ± 1.7 pS ($n = 18$) obtained in Na^+-ASW. When the solution perfusing the patches was changed to Tris- or NMDG-ASW, which in whole-cell experiments resulted in either no response or a transient response, single-channel conductances were decreased by approximately two-thirds. The mean slope conductance obtained for cation channels was reduced from 29.1 pS to 10.4 ± 1.9 pS ($n = 3$) and 8.9 ± 2.1 pS ($n = 3$) in ASW containing Tris and NMDG as the dominant monovalent cation, respectively. As will be described below, the currents remaining in the Tris- and NMDG-ASW solutions, which correspond to the extracellular solutions in

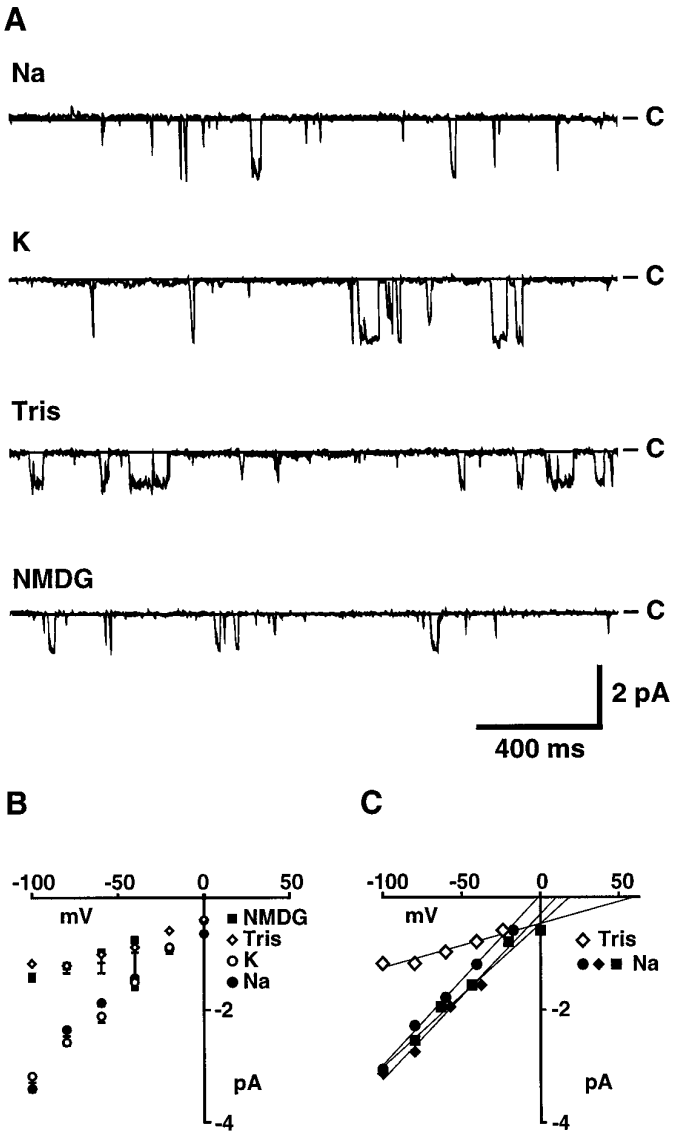

Figure 6. Selectivity of bag cell neuron cation channels for monovalent cations. The Na^+ of ASW was substituted with an equimolar amount of the indicated cations to allow comparison with measurements of the whole-cell cation current. Solution changes were accomplished using a gravity-driven multibarrel perfusion system, and outside/out patches were moved from the mouth of one barrel to the next. *A*, Cation channel activity recorded at a holding potential of −60 mV in outside/out patches perfused with ASW containing Na^+, K^+, Tris, or NMDG as the dominant monovalent cation, as indicated. *B*, Average open-channel current–voltage relation for each test solution, as indicated. The number of observations contributing to each point going from −100 to 0 mV in 20 mV increments are: for Na-ASW, 7, 10, 16, 12, 8, and 3; for K-ASW, 3, 7, 5, 5, 4, and 2; for Tris-ASW, 1, 3, 3, 2, 2, and 1; for NMDG-ASW, 3, 3, 6, 3, 0, and 0. Single-channel conductances, as determined by straight-line fits to the points obtained over the −100 to 0 mV range for each channel (see insert for examples) and then averaged, were 29.1 ± 1.7 (n = 18), 30.5 ± 1.5 (n = 6), 10.4 ± 1.9 (n = 3), and 8.9 ± 2.1 (n = 3) for Na^+, K^+, Tris, and NMDG containing ASW, respectively. *C*, Examples of the open-channel current–voltage relations for individual channels showing straight-line fits and extrapolated reversal potentials.

the whole-cell experiments (Fig. 5), are likely to be carried in part by Ca^{2+} ions. Nevertheless, the above results suggest that the relative permeability for the monovalent cations tested follows the sequence K ≅ Na ≫ Tris > NMDG and that Tris and NMDG are either less permeant than Na^+ or not at all permeant. No change in the amplitude of unitary currents was observed when inside/out patches were perfused with an intracellular solution in which KCl replaced all K-aspartate (n = 3), indicating that anions are not measurably permeant.

The reversal potential, which is sensitive to the concentrations of all permeant ions in the intracellular and extracellular solutions, also can provide information on the ion selectivity of a channel (Goldman, 1943; Hodgkin and Katz, 1949; Lewis, 1979). Because of the prevalence of voltage-sensitive K channels, however, we were unable to distinguish clearly cation channels at positive potentials and therefore did not attempt to determine their reversal potential directly. We were able, however, to estimate reversal potentials by extrapolation of the inward currents measured at negative potentials. Because each channel was not tested at every voltage (see legend for Fig. 6*B*), average reversal potentials were determined by straight-line fits to the data for each channel and then averaged across channels. Examples of individual fits are shown in Figure 6*C*. The average reversal potential obtained in this way (8.6 ± 4.2 mV; n = 18) is more accurate than that obtained by extrapolation via the average data points shown in Figure 6*B* (~25 mV), because the latter method assigns each point equal weight regardless of the number of observations. Even so, given possible rectification in the open-channel current–voltage relation, these extrapolated reversal potentials are only suggestive of the actual shifts that occur. In the experiments above, in which the Na^+ of ASW was substituted by an equimolar amount of the other monovalent test ions, both K^+ (10.4 mM) and Ca^{2+} (11 mM) were present throughout. Given that the cation channel is nearly equally permeable to K^+ and Na^+, a negative shift in the reversal potential toward the equilibrium potential for K^+ ions would be expected for test solutions in which a less permeant ion was substituted for Na^+. Instead, the average reversal potentials in Tris and NMDG, extrapolated from current measurements over the −100 to 0 mV range, seemed shifted to more depolarized values [from 8.6 ± 4.2 (n = 18) to 35.7 ± 12.2 (n = 3) and 35.5 ± 7.5 mV (n = 3), respectively]. One explanation of this shift is that Ca^{2+} ions also might be permeant and that the permeability of the channel to Ca^{2+} is substantially increased in the absence of Na^+. In agreement, when the solution perfusing the patch was changed to ASW (in which 66 mM Ba^{2+} was substituted for the Ca^{2+} and Mg^{2+} normally present), the slope conductance measured over −100 to −20 mV increased from a control value of 30 to 86 pS for the channel shown in Figure 7. Similar results were observed in two other patches. When only Ca^{2+} was substituted by Ba^{2+} (11 mM), the average slope conductance of cation channels increased from the average control value of 29.1 pS to 36 ± 3.2 pS (n = 3).

Ca^{2+} sensitivity

In experiments attempting to examine the effects of Ca^{2+} substitution on the whole-cell current, the response to CtVm often was eliminated (n = 8 of 11). Because Ca^{2+}-dependence is a property associated with a number of nonspecific cation channels (for review, see Partridge and Swandulla, 1988), we sought to determine whether intracellular Ca^{2+} levels regulate the CtVm-induced depolarization. For these experiments, we used the whole-cell patch-clamp technique, which permitted intracellular Ca^{2+} levels to be buffered by the EGTA included in the pipette solution. Membrane potentials were monitored for ~10 min to verify their stability in control conditions and to allow EGTA to diffuse into bag cell neurons. Figure 8*A* compares the average

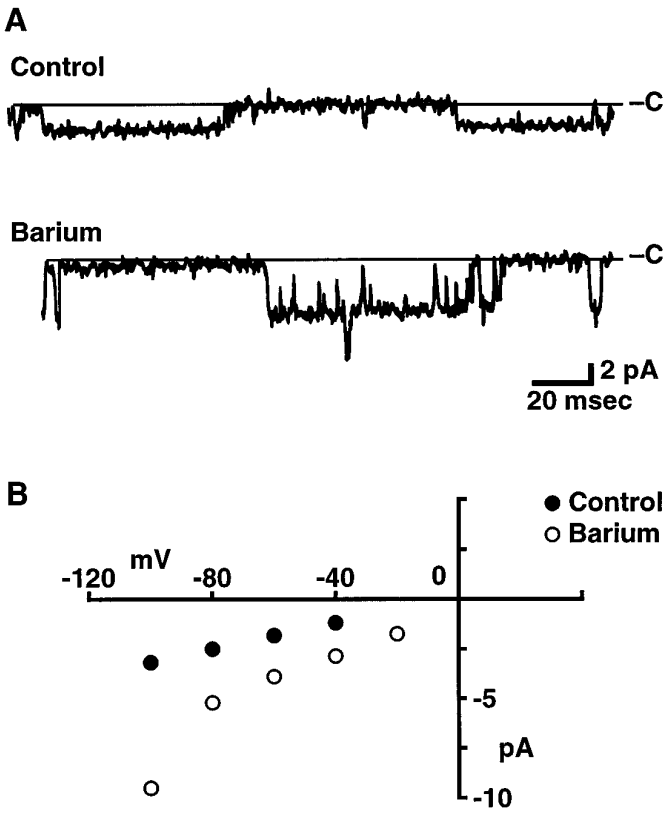

Figure 7. Selectivity of bag cell neuron cation channels for divalent cations. *A*, Representative steady-state recordings of cation channel activity in an outside/out patch perfused with control ASW and ASW in which the Ca^{2+} and Mg^{2+} were substituted by an equimolar amount of Ba^{2+}. The holding potential was −60 mV. Two current levels were observed (see *bottom* trace), indicating the presence of at least two channels in the patch. *B*, Open channel current–voltage relation for the first level of current observed in the patch shown in *A*.

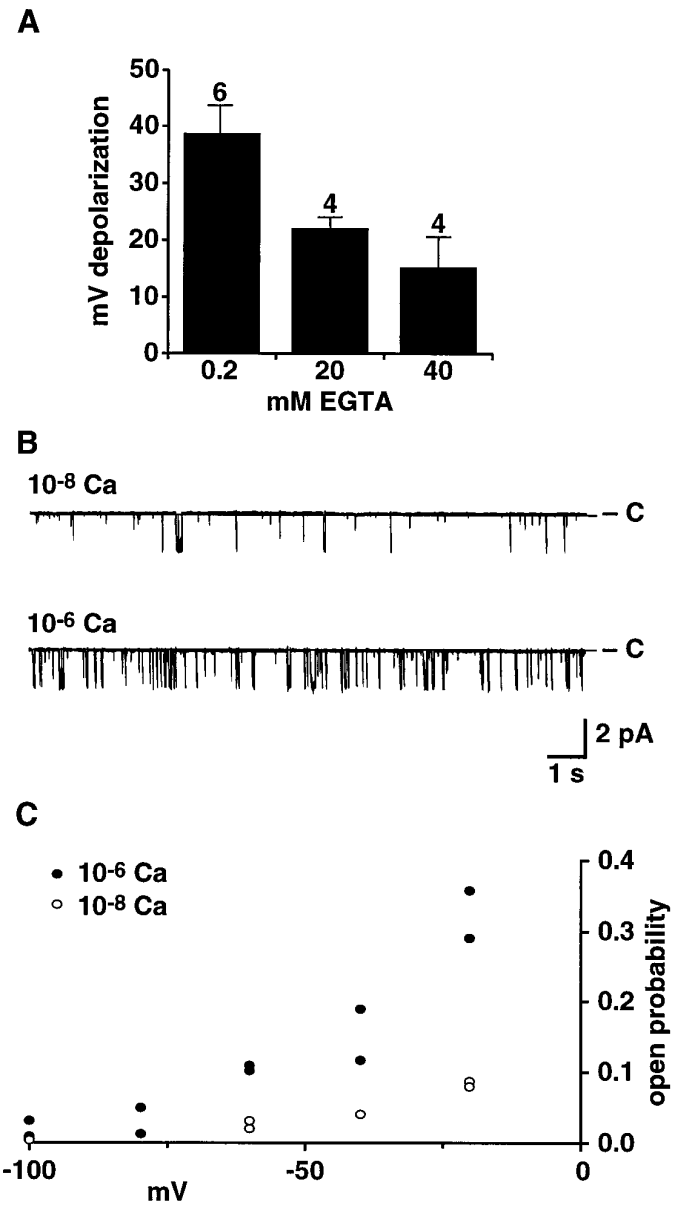

Figure 8. Ca^{2+} sensitivity of the CtVm-induced depolarization and cation channel activity. *A*, Decreasing intracellular Ca^{2+} levels (by increasing intracellular EGTA) decreases the magnitude of depolarizations observed in response to application of CtVm (100 μg/ml) in whole-cell patch-clamp recordings of bag cell neurons. To permit the diffusion of EGTA from the patch pipette into bag cell neurons, ~10 min were allowed between rupture of the membrane by the patch pipette and application of CtVm. The intracellular solution in the patch pipette contained 5 mM $MgCl_2$ and either 0.2 mM EGTA and 0 mM $CaCl_2$; 20 mM EGTA and 4.14 mM $CaCl_2$ (for a calculated free Ca^{2+} concentration of 3.5×10^{-8} M); or 40 mM EGTA and 4.14 mM $CaCl_2$ (for a calculated free Ca^{2+} concentration of 1.5×10^{-8} M). The numbers of cells examined for the 0.2, 20, and 40 mM EGTA conditions were 6, 4, and 4, respectively. *B*, Representative steady-state recordings of cation channel activity in an inside/out patch perfused with an intracellular solution containing either 10^{-8} or 10^{-6} M free Ca^{2+}, as indicated. The holding potential was −60 mV. *C*, Shift in voltage-dependence of cation channel activation with changes in intracellular Ca^{2+}. *Points* represent the P_o obtained for two inside/out patches containing cation channels with a similar starting level of activity (i.e., at a holding potential of −60 mV and 10^{-6} Ca^{2+}).

magnitude of the CtVm-induced depolarizations observed when the pipette solution contained either 0.2, 20, or 40 mM EGTA. Although the CtVm-induced depolarizations were not eliminated at free $[Ca^{2+}]_i$ concentrations that eliminate the Ca^{2+}-activated K currents of bag cell neurons (20 mM EGTA in Fig. 8*A*) (Strong and Kaczmarek, 1986), the magnitudes of the observed depolarizations were reduced by nearly half ($n = 4$), and further reductions in magnitude were observed on a doubling of the EGTA concentration from 20 to 40 mM ($n = 4$).

More direct evidence for the Ca^{2+} sensitivity of the cation channel was obtained in recordings from excised inside/out patches of bag cell neurons. Figure 8*B* shows recordings of single cation channel activity when the solution perfusing the intracellular face of the membrane contained either 10^{-8} or 10^{-6} M free Ca^{2+}. At 10^{-8} M free Ca^{2+} and a holding potential of −60 mV, the measured single-channel P_o was 0.03. Increasing the free Ca^{2+} to 10^{-6} M resulted in an increase in the activity of the channel, as reflected by the more than threefold increase in P_o to 0.1. Although starting P_o values varied across cation channels, similar increases in channel activity after increases in $[Ca^{2+}]_i$ were observed in all 14 of the patches tested and were independent of the order in which the Ca^{2+} concentrations were presented. In the three cases in which the same Ca^{2+} concentration was presented more than once, the changes in P_o were reversible. In no case was channel activity completely eliminated by lowering $[Ca^{2+}]_i$, even

to 10^{-9} M Ca^{2+}. If it is assumed that changes in $[Ca^{2+}]_i$ did not affect the slope of the voltage-dependence curve, a preliminary examination of the change in the voltage-dependence of the single channel P_o as a function of $[Ca^{2+}]_i$ suggests a shift in the activation of the cation channel of 40 to 50 mV in the hyperpolarizing direction for a change in $[Ca^{2+}]_i$ from 10^{-8} to 10^{-6} M free Ca^{2+} (Fig. 8*C*). A shift of ~70 mV is observed for Ca^{2+}-activated K channels for a similar shift in Ca^{2+} concentration (Moczydlowski and Latorre, 1983).

DISCUSSION

Slow inward currents contribute to the plasticity of neurons by regulating firing patterns and levels of spontaneous activity and are prevalent in both mammalian and molluscan neurons. The results of the present study provide evidence that a Ca^{2+}-sensitive nonspecific cation channel carries the slow inward current observed in bag cell neurons after treatment with CtVm and suggest that this current underlies CtVm-induced depolarization and repetitive firing. The cation channel was the only channel observed in any patch configuration with characteristics similar to those of the whole-cell current. Previous studies on bursting neurons have identified the nonspecific cation channels presumed to underlie bursting primarily on the basis of their inward elementary currents and the increases in channel activity seen in response to the increases in either intracellular Ca^{2+} or cAMP, which activate slow inward currents in whole-cell recordings (Green and Gillette, 1983; Partridge and Swandulla, 1987; Sudlow et al., 1993). Both the whole-cell slow inward current and cation channel of *Aplysia* bag cell neurons are activated by CtVm, are active over a similar voltage range, are blocked by high concentrations of TTX, and are sensitive to intracellular Ca^{2+} levels. In addition, the cation channels of bag cell neurons are permeable to both monovalent and divalent cations as observed for ligand-gated nonspecific cation currents (Mayer and Westbrook, 1987), and the selectivity of both the whole-cell current and cation channel for monovalent cations follows the sequence $K \cong Na \gg Tris > NMDG$. Further characterization of the nonspecific cation channels of different neurons and computer modeling will be required to determine whether differences in channel properties and modulation contribute to the difference between an afterdischarge and bursting.

Despite the overall similarity of the whole-cell current and the cation channel of excised patches, some differences deserve note. First, the reversal potential extrapolated from cation channel currents was, at best, ~10 mV positive to that observed for the TTX-sensitive whole-cell current. A number of plausible explanations of this difference exist, including a difference in the composition of the intracellular solution and the bag cell neuron cytoplasm, a slow rundown or inactivation of an outward current during the time needed to obtain the TTX-sensitive difference current, or a voltage-dependence in the block of the cation current by TTX so that less current is blocked at increasingly depolarized potentials. Because a significant component of the bag cell neuron K current is resistant to traditional K channel blockers, we were unable to isolate the cation current at positive potentials to test the latter hypothesis.

Second, the conductance of cation channels in Tris- and NMDG-ASW was reduced by approximately two-thirds, whereas the CtVm-induced current often appeared to be eliminated by the same substitutions. A likely explanation is that the CtVm response in whole-cell experiments is significantly attenuated in duration, making detection of the current difficult given the current subtraction protocol used. Recent work has suggested that the activity of kinases and phosphatases can be affected by changes in ion flux (Lanius et al., 1993; Holmes et al., 1995); whether an ion-dependent change in the activity of second messengers affects the duration of the response to CtVm in our experiments is unknown, but it is an interesting possibility.

Third, despite the evidence that CtVm activates both the channel and the whole-cell current, cation channels were not observed in cell-attached patches even after application of CtVm. The inability to detect cation channels in cell-attached patches may be a consequence of the deformation of the surrounding membrane by the pipette. A similar requirement for the integrity of channels and their surrounding membrane has been reported for the modulation of bag cell neuron Ca channels (Strong et al., 1987). Not only are cation channels highly clustered, but a tyrosine phosphatase and serine/threonine kinase appear closely associated (Wilson and Kaczmarek, 1992, 1993); the pressure of the pipette in cell-attached patches may deform the spatial relationship between enzymes and cation channels. Similarly, subplasma membrane organelles and their ability to release Ca^{2+} also may be affected by membrane deformation. Once the patch is excised, the effects on the membrane immediately outside the pipette are no longer present, and this excision may allow the remaining channels, enzymes, and organelles to function normally.

A fourth difference concerns the voltage-dependence of the whole-cell current and cation channel. At potentials negative to −40 mV, channels exhibited a higher level of activity than expected from examination of the whole-cell current. Both phosphorylation by cAMP-dependent protein kinase (PKA) and intracellular Ca^{2+} levels may account for this difference. PKA decreases the P_o of continuously active cation channels by 40% at holding potentials of −60 mV, and preliminary evidence suggests that this effect is voltage-dependent: the reduction in P_o becomes more extreme as the potential is shifted to more hyperpolarized values (Wilson and Kaczmarek, 1993; our unpublished observations). Because CtVm elicits afterdischarge-like activity and because intracellular cAMP levels are known to increase at the onset of the afterdischarge (Kaczmarek et al., 1978), our whole-cell measurements most likely reflect cation channel activity in the PKA-phosphorylated state. In addition, the cation channels are Ca^{2+}-sensitive. In the present experiments, the voltage-dependence of the cation channel P_o was assessed at free Ca^{2+} concentrations of 10^{-6} M. Because the intracellular Ca^{2+} concentration of bag cell neurons is $\sim 1 \times 10^{-7}$ to 2×10^{-7} M near the plasma membrane (Fink et al., 1988), cation channels would be less active at hyperpolarized potentials.

Like slow inward currents of a number of other molluscan neurons (Connor and Hockberger, 1984; Swandulla and Lux, 1985; Kirk and Scheller, 1986; Kehoe, 1990), the cation current of bag cell neurons does not contribute to the current–voltage relation of quiescent cells but requires stimulation to be observed. The use of CtVm in the present study allowed the identification and characterization of a channel and current that may contribute to the onset of the afterdischarge *in vivo*. The effects of CtVm appear distinct from those observed in other *Aplysia* neurons (Hasson et al., 1993) in that, in the present experiments, the purified King Kong peptide failed to reproduce the effects of the extract. The response to the King Kong peptide in the study of Hasson et al. (1993) also differed from that observed in the present study in its kinetics and its insensitivity to Ca^{2+} and TTX. The stimuli normally triggering the afterdischarge *in vivo* may include both neuropeptides released by the pleuroabdominal connective nerve presynaptic to bag cell neurons and autoactive

peptides released by bag cell neurons in response to their initial stimulation. Both atrial gland peptides and the α-, β-, and γ-bag cell peptides trigger afterdischarge-like activity when they are applied to acutely isolated ganglia (Heller et al., 1980; Brown and Mayeri, 1989). Although it is not clear at what point the mechanisms of electrically stimulated and CtVm-induced discharges converge, the observed discharges are indistinguishable to the extent tested. Therefore, it is plausible that a component of CtVm binds to the receptor for the neuropeptide normally triggering the afterdischarge. At the other extreme, the neuropeptides released *in vivo* may activate channels in addition to or in lieu of the cation channel we describe.

Because CtVm was able to increase cation channel activity in patch-cramming experiments without direct access to the extracellular face of cation channels, channel activation by CtVm seems to occur indirectly via the activation of intracellular messengers. Likely candidates include intracellular cAMP and Ca^{2+}, which increase at the onset of electrically stimulated afterdischarges (Kaczmarek et al., 1978; Fisher et al., 1994). Cation channel activity is upregulated by increases in intracellular Ca^{2+}, by PKA acting through an endogenous tyrosine phosphatase (Wilson and Kaczmarek, 1993), and by hydrolyzable nucleotides (Wilson and Kaczmarek, 1992). In the patch-cramming experiments of the present study, application of CtVm caused cation channels to transit from a bursting to a continuous high-activity mode. In cell-free patches, this transition previously has been shown to be caused by activation of a PKA-regulated tyrosine phosphatase closely associated with the cation channel protein (Wilson and Kaczmarek, 1993). The transition from the bursting to high-activity mode can increase the fraction of time cation channels spend in the open state by as much as 85-fold and, thus, is of sufficient magnitude to account for the depolarization triggering the onset of the discharge. From the effect of CtVm on cation channels exhibiting a continuous but low level of activity, however, it seems likely that CtVm acts via more than one second messenger. To date, tyrosine phosphatases are the only second messengers that have been observed to cause the transition from the bursting to continuously active mode. Because activation of the endogenous tyrosine phosphatase does not result in an increase of the P_o of channels in the continuously active mode, it seems probable that another second messenger is responsible for the CtVm-induced increase in the P_o of channels exhibiting this latter gating mode. The observed transition from low to high activity in continuously active channels may be a result of increases in intracellular Ca^{2+}, increases in the levels of hydrolyzable nucleotides, or activation of an as yet unidentified additional intracellular messenger. Whether the multiple effects of CtVm are a consequence of a single peptide or multiple peptides with distinct actions remains a subject for future investigation.

In addition to differences in their voltage-dependence and their regulation by Ca^{2+} and cAMP (Partridge and Swandulla, 1988), nonspecific cation currents seem to vary considerably in their time course of activation and inactivation, selectivity, and sensitivity to block by TTX. At least some of these differences may be a consequence of the states of the neurons when examined (e.g., which intracellular messengers are present and activated), the presence of other currents activated by the same stimuli, and variations in methods (e.g., TTX concentrations). Nonetheless, nonspecific cation currents seem to be one of the most flexible classes of currents when characterized by the above criteria. In a manner akin to ligand-gated channels, the primary classifying feature may be the predominant intracellular messenger-regulating channel activity. As characterization of these channels progresses, it will be interesting to determine which features serve to distinguish among family members at the molecular level.

REFERENCES

Alonso A, Llinas RR (1989) Subthreshold Na^+-dependent theta-like rhythmicity in stellate cells of entorhinal cortex layer II. Nature 342:175–177.

Brown RO, Mayeri E (1989) Positive feedback by autoexcitatory neuropeptides in neuroendocrine bag cells of *Aplysia*. J Neurosci 9:1443–1451.

Chang D, Hsieh PS, Dawson DC (1988) Calcium: a program in BASIC for calculating the composition of solutions with specified free concentrations of calcium, magnesium, and other divalent cations. Comput Biol Med 18:351–366.

Colquhoun D, Neher E, Reuter H, Stevens CF (1981) Inward current channels activated by intracellular Ca in cultured cardiac cells. Nature 294:752–754.

Connor JA, Hockberger P (1984) A novel sodium current induced by injection of cyclic nucleotides into gastropod neurones. J Physiol (Lond) 354:139–162.

Cruz LJ, Corpus G, Olivera BM (1976) A preliminary study of *Conus* venom protein. Veliger 18:302–308.

Eckert R, Lux HD (1976) A voltage-sensitive persistent calcium conductance in neuronal somata of *Helix*. J Physiol (Lond) 254:129–151.

Fink LA, Connor JA, Kaczmarek LK (1988) Inositol trisphosphate releases intracellularly stored calcium and modulates ion channels in molluscan neurons. J Neurosci 8:2544–2555.

Fisher TE, Levi S, Kaczmarek LK (1994) Transient changes in intracellular calcium associated with a prolonged increase in excitability in neurons of *Aplysia californica*. J Neurophysiol 71:1254–1257.

Goldman DE (1943) Potential, impedance, and rectification in membranes. J Gen Physiol 27:37–60.

Gray WR, Olivera BM, Cruz LJ (1988) Peptide toxins from venomous *Conus* snails. Annu Rev Biochem 57:665–700.

Green DJ, Gillette R (1983) Patch- and voltage-clamp analysis of cyclic AMP-stimulated inward current underlying neurone bursting. Nature 306:784–785.

Hasson A, Fainzilber M, Gordon D, Zlotkin E, Spira M (1993) Alteration of sodium currents by new peptide toxins from the venom of a molluscivorous *Conus* snail. Eur J Neurosci 5:56–64.

Heller E, Kaczmarek LK, Hunkapiller MW, Hood LE, Strumwasser F (1980) Purification and primary structure of two neuroactive peptides that cause bag cell afterdischarge and egg-laying in *Aplysia*. Proc Natl Acad Sci USA 77:2328–2332.

Hillyard DR, Olivera BM, Woodward S, Corpuz GP, Gray WR, Ramilo CA, Cruz LJ (1989) A molluscivorous *Conus* toxin: conserved frameworks in conotoxins. Biochemistry 28:358–361.

Hoehn K, Watson TWJ, MacVicar BA (1993) A novel tetrodotoxin-insensitive, slow sodium current in striatal and hippocampal neurons. Neuron 10:543–552.

Hodgkin AL, Katz B (1949) The effect of sodium ions on the electrical activity of the giant axon of the squid. J Physiol (Lond) 108:37–77.

Hofmeier G, Lux HD (1981) The time courses of intracellular free calcium and related electrical effects after injection of $CaCl_2$ into neurons of the snail, *Helix pomatia*. Pflügers Arch 391:242–251.

Holmes TC, Berman KS, Bowlby MR, Levitan IB (1995) Expression of the voltage-dependent potassium channel Kv1.3 decreases cellular tyrosine phosphorylation. Soc Neurosci Abstr 7:719.

Kaczmarek LK, Jennings KR, Strumwasser F (1978) Neurotransmitter modulation, phosphodiesterase inhibitor effects, and cyclic AMP correlates of afterdischarge in peptidergic neurites. Proc Natl Acad Sci USA 75:5200–5204.

Kaczmarek LK, Finbow M, Revel JP, Strumwasser F (1979) The morphology and coupling of *Aplysia* bag cells within the abdominal ganglion and in cell culture. J Neurobiol 10:535–550.

Kauer JA, Kaczmarek LK (1985) Peptidergic neurons of *Aplysia* lose their response to cyclic adenosine 3′,5′-monophosphate during a prolonged refractory period. J Neurosci 5:1339–1345.

Kehoe J (1990) Cyclic AMP-induced slow inward current in depolarized neurons of *Aplysia californica*. J Neurosci 10:3194–3207.

Kirk MD, Scheller RH (1986) Egg-laying hormone of *Aplysia* induces a voltage-dependent slow inward current carried by Na^+ in an identified motoneuron. Proc Natl Acad Sci USA 83:3017–3021.

Kramer RH (1990) Patch cramming: monitoring intracellular messengers in intact cells with membrane patches containing detector ion channels. Neuron 2:335–431.

Kramer RH, Zucker RS (1985) Calcium-dependent inward current in *Aplysia* bursting pace-maker neurones. J Physiol (Lond) 362:107–130.

Kupfermann I, Kandel ER (1970) Electrophysiological properties and functional interconnections of two symmetrical neurosecretory clusters (bag cells) in abdominal ganglion of *Aplysia*. J Neurophysiol 33:865–876.

Lanius RA, Pasqualotto BA, Shaw CA (1993) A novel mechanism of AMPA receptor regulation: ionically triggered kinases and phosphatases. NeuroReport 4:795–798.

Lanthorn T, Storm J, Anderson P (1984) Current-to-frequency transduction in CA1 hippocampal pyramidal cells: slow prepotentials dominate the primary range firing. Exp Brain Res 53:431–443.

Lewis CA (1979) Ion-concentration dependence of the reversal potential and the single channel conductance of ion channels at the frog neuromuscular junction. J Physiol (Lond) 286:417–445.

Lewis DV (1984) Spike aftercurrents in R15 of *Aplysia*: their relationship to slow inward current and calcium influx. J Neurophysiol 51:387–403.

Mayer ML, Westbrook GL (1987) Permeation and block of *N*-methyl-D-aspartic acid receptor channels by divalent cations in mouse cultured central neurones. J Physiol (Lond) 394:501–527.

Moczydlowski E, Latorre R (1983) Gating kinetics of Ca^{2+}-activated K^+ channels from rat muscle incorporated into planar bilayers: evidence for two voltage-dependent binding reactions. J Gen Physiol 82:511–542.

Olivera BM, Rivier J, Clark C, Ramilo CA, Corpuz GP, Abogadie FC, Mena EE, Woodward SR, Hillyard DR, Cruz LJ (1990) Diversity of *Conus* neuropeptides. Science 249:257–263.

Partridge LD, Swandulla D (1987) Single Ca-activated cation channels in bursting neurons of *Helix*. Pflügers Arch 410:627–631.

Partridge LD, Swandulla D (1988) Calcium-activated non-specific cation channels. Trends Neurosci 11:69–72.

Partridge LD, Thompson SH, Smith SJ, Connor JA (1979) Current–voltage relationships of repetitively firing neurons. Brain Res 164:69–79.

Reuter H (1984) Ion channels in cardiac cell membranes. Annu Rev Physiol 46:473–484.

Stafstrom CE, Schwindt PC, Chubb MC, Crill WE (1985) Properties of persistent sodium conductance and calcium conductance of layer V neurons from cat sensorimotor cortex in vitro. J Neurophysiol 53:153–170.

Strong JA, Kaczmarek LK (1986) Multiple components of delayed potassium current in peptidergic neurons of *Aplysia*: modulation by an activator of adenylate cyclase. J Neurosci 6:814–822.

Strong JA, Fox AP, Tsien RW, Kaczmarek LK (1987) Stimulation of protein kinase C recruits covert calcium channels in *Aplysia* bag cell neurons. Nature 325:714–717.

Sudlow LC, Huang R-C, Green D, Gillette R (1993) cAMP-activated Na^+ current of molluscan neurons is resistant to kinase inhibitors and is gated by cAMP in the isolated patch. J Neurosci 13:5188–5193.

Swandulla D, Lux HD (1985) Activation of a nonspecific cation conductance by intracellular Ca^{2+} elevation in bursting pacemaker neurons of *Helix pomatia*. J Neurophysiol 54:1430–1443.

Wilson GF, Kaczmarek LK (1992) Modulation of an *Aplysia* divalent-permeable cation channel by endogenous kinase and the catalytic subunit of protein kinase A. Soc Neurosci Abstr 4:253.

Wilson GF, Kaczmarek LK (1993) Mode-switching of a voltage-gated cation channel is mediated by a protein kinase A-regulated tyrosine phosphatase. Nature 366:433–438.

Wilson WA, Wachtel H (1974) Negative resistance characteristic essential for the maintenance of slow oscillations in bursting neurons. Science 186:932–934.

Yellen G (1982) Single Ca^{2+}-activated nonselective cation channels in neuroblastoma. Nature 296:357–359.